Published in final edited form as:
Am J Hematol. 2009 July ; 84(7): 401–407. doi:10.1002/ajh.21444.

Tumor-associated macrophages infiltrate plasmacytomas and can serve as cell carriers for oncolytic measles virotherapy of disseminated myeloma

Kah-Whye Peng[1], **Ahmet Dogan**[2], **Julie Vrana**[2], **Chunsheng Liu**[1], **Hooi T. Ong**[1], **Shaji Kumar**[3], **Angela Dispenzieri**[3], **Allan B. Dietz**[4], and **Stephen J. Russell**[1,3,*]

[1]Department of Molecular Medicine, Mayo Clinic, Rochester, Minnesota

[2]Department of Anatomic Pathology, Mayo Clinic, Rochester, Minnesota

[3]Division of Hematology, Mayo Clinic, Rochester, Minnesota

[4]Department of Transfusion Medicine, Mayo Clinic, Rochester, Minnesota

Abstract

In multiple myeloma, some of the neoplastic plasma cells are diffusely dispersed among the normal bone marrow cells (bone marrow resident), whereas others are located in discrete, well-vascularized solid tumors (plasmacytomas) that may originate in bone or soft tissue. Interactions between bone marrow-resident myeloma cells and bone marrow stromal cells (BMSCs) are important determinants of myeloma pathogenesis. However, little is known of the factors sustaining myeloma growth and cell viability at the centers of expanding plasmacytomas, where there are no BMSCs. Histologic sections of 22 plasmacytomas from myeloma patients were examined after immunostaining. Abundant CD68+, CD163+, S100-negative macrophage infiltrates were identified in all tumors, accompanied by scattered collections of CD3+ T lymphocytes. The CD68+ tumor-associated macrophages (TAM) accounted for 2– 12% of nucleated cells and were evenly distributed through the parenchyma. The TAM generally had dendritic morphology, and each dendrite was in close contact with multiple plasma cells. In some cases, the TAM were strikingly clustered around CD34 + blood vessels. To determine whether cells of the monocytic lineage might be exploitable as carriers for delivery of therapeutic agents to plasmacytomas, primary human CD14+ cells were infected with oncolytic measles virus and administered intravenously to mice bearing KAS6/1 human myeloma xenografts. The cell carriers localized to KAS6/1 tumors, where they transferred MV infection to myeloma cells and prolonged the survival of mice bearing disseminated human myeloma disease. Thus, TAM are a universal stromal component of the plasmacytomas of myeloma patients and may offer a promising new target for therapeutic exploitation.

Introduction

Multiple myeloma is a disseminated malignancy of antibody-secreting plasma cells that are either (i) diffusely admixed with normal bone marrow cells throughout the red marrow spaces of the axial and proximal appendicular skeleton or (ii) located in discrete, well-vascularized plasmacytomas [1]. The appearance and expansion of skeletal plasmacytomas is one of the defining characteristics of progression from MGUS to multiple myeloma [2]. The interactions

*Correspondence to: Stephen J. Russell, MD, PhD, Mayo Clinic, 200 First Street SW, Rochester, MN 55905. sjr@mayo.edu.

Conflict of interest: Nothing to report.

of bone marrow-resident myeloma cells with osteoclasts, osteoblasts, dendritic cells (DC), and other bone marrow stromal cells (BMSCs) have been studied extensively and are known to contribute significantly to myeloma pathogenesis [3–6]. However, although the interactions between bone marrow cells and myeloma cells are clearly important for some aspects of myeloma pathogenesis, they cannot be of major relevance at the centers of expanding plasmacytomas because these sites are devoid of osteoclasts, osteoblasts, and other BMSCs. It is now well known that plasmacytomas have a high density of new blood vessels [7], but surprisingly there have been no previous publications documenting the presence or distribution of other cell types at the centers of plasmacytomas. Histologic examination of other solid and hematologic tumors indicates that they are often infiltrated by tumor-associated macrophages (TAMs) [8–12]. We therefore obtained archived paraffin blocks of plasmacytoma biopsies from 22 patients with a diagnosis of multiple myeloma and immunostained the sections with antibodies to macrophage and dendritic cell markers CD68, CD163, and S100. There were abundant CD68+, CD163+ cells in the human plasmacytomas. Because chemoattractants produced by the malignant and stromal cells in the tumor recruit monocytes from the blood-stream and stimulate them to differentiate into TAMs [9], we also sought to explore the possibility that cells from monocytic lineage might serve as carriers for intravenous delivery of oncolytic measles virus to sites of tumor growth.

Results

Plasmacytomas are diffusely infiltrated with macrophages

We obtained archived paraffin blocks of 22 plasmacytoma biopsies from patients with a diagnosis of multiple myeloma and immunostained the sections with antibodies to macrophage and dendritic cell markers CD68, CD163, and S100. We focused our initial studies on cells of monocytic origin because other members of this lineage (osteoclasts in particular) have been shown to sustain the growth and viability of myeloma cells diffusely infiltrating the bone marrow [6]. As expected, hematoxylin and eosin–stained sections revealed only monotonous sheets of plasma cells interspersed with numerous small blood vessels (Fig. 1A). However, immunohistochemical staining with anti-human CD68 (Fig. 1B–I) and anti-human CD163 antibodies (data not shown) revealed uniformly dispersed macrophage infiltrates throughout the parenchyma of every plasmacytoma examined. In contrast to macrophages, CD3-positive T-cell infiltrates were less uniformly distributed in these plasmacytomas (Fig. 1J–L). The percentage of CD3-positive T lymphocytes ranged from 0.6 to 6% of nucleated cells in these samples (2.7 + 2.8%, mean ± SD) For each case examined, the number of CD68-positive cells per 400× high-power field (Fig. 2A) was counted and expressed as a percentage of the total number of cells in the same field of view (Fig. 2B). Ten representative high-power fields were counted for each plasmacytoma sample. As shown in Fig. 2B, from 2 to 12% of the cells in these plasmacytomas were identified as CD68-positive TAMs. In most of the cases examined, the CD68 cells had dendritic morphology (Fig. 1 and Fig. 2), but stained negative for the dendritic cell marker S100 (data not shown). Each dendrite was seen to be closely associated with multiple surrounding plasma cells (Fig. 2A). To investigate whether human plasmacytomas xenografted in mice become infiltrated with mouse TAMs, we explanted subcutaneous KAS6/1 and MM1 xenografts from SCID mice and immunostained them using an anti-mouse CD68 antibody. As shown in Supporting Information Fig. 1, these tumors were heavily infiltrated with CD68-positive murine macrophages, indicating that murine monocytes are recruited efficiently into these tumors (Supporting Information Fig. 1).

Additional Supporting Information may be found in the online version of this article.

Relationship between TAMs and tumor neovessels

TAM have been identified in a wide range of tumor types [8–13] and have been shown to contribute to tumor growth and survival in several ways, one of which is to promote the formation of new tumor blood vessels (neoangiogenesis) [14]. We therefore sought to determine the microanatomical location of the plasmacytoma-infiltrating TAMs in relation to tumor blood vessels. Plasmacytoma sections were double stained with antibodies to CD68 and to the neovessel marker CD34, which, in contrast to CD31, is absent from the surfaces of neoplastic plasma cells [15]. Anti-CD34 antibodies have been used in several previous publications for the evaluation of microvessel density in plasmacytomas [7,16]. CD34+ microvessel density and numbers of CD68 TAMs were counted and there was no correlation between these two parameters (data not shown). However, we noted that there were two different patterns of TAM infiltration in relation to CD34 microvessels (Fig. 3). In most of the cases (16 of 20), the CD68-positive macrophages and the CD34-positive blood vessels were randomly distributed throughout the tumor parenchyma and did not show any obvious colocalization (Fig. 3A, B). However, in four of the plasmacytomas, there was a prominent subpopulation of TAMs that showed a striking association with the tumor neovessels (Fig. 3C–F). It will be interesting to determine whether these cells are contributing to the process of tumor angiogenesis. Bone marrow-resident macrophages from patients with multiple myeloma were recently shown to be capable of vasculogenic mimicry [17]. Careful analysis of the plasmacytoma sections shown in Fig. 3 provides evidence that TAM at this site may also be capable of vascular mimicry.

Monocyte-derived cells can be infected by oncolytic measles virus

Based on the observation that plasmacytomas are heavily infiltrated with TAMs, which are recruited from the circulation as monocytes by the tumor, we hypothesized that it might be feasible to use monocyte-derived cells as carriers for delivery of oncolytic viruses via the bloodstream to sites of tumor growth. Human leukocytes retained in the leukoreduction system chambers after apheresis were collected and the mononuclear fraction was purified through a density gradient solution. CD14+ cells were isolated using CD14-specific immunomagnetic reagents. Cells at different stages of maturation were used to determine relative susceptibility to virus infection, ability to transfer the virus to myeloma cells, and biodistribution to site of tumor growth. Thus, CD14+ monocytes were used immediately in infection assays or cultured in granulocyte-macrophage colony stimulating factor (GM-CSF) containing media for 3 days to yield immature DCs (iDC) or for another 3 days in the same media supplemented with tumor necrosis factor-α and prostaglandin E2 (PGE2) added to yield mature DCs (mDC).

We first determined the susceptibility of these cells at different maturation stages to measles infection. Cells from normal blood donors were infected with MV-eGFP (MOI 1.0) for 2 hr in Opti-MEM after which standard media containing a fusion inhibitory peptide (FIP) was added. The presence of FIP prevents syncytia formation, allowing analysis of single virus-infected cells by flow cytometry. As shown in Fig. 4A, cells of the CD14 monocyte-derived lineage from four representative donors are highly susceptible to MV-eGFP infection, irrespective of their maturation status, with infectivities ranging from 40 to 80% at a multiplicity of infection of 1.0. To determine the extent of heterofusion and virus transfer between the infected cell carriers and myeloma cells, MV-Luc–infected DiO-labeled (green fluorescent) monocytes, iDCs or mDCs, were cocultured with human KAS 6/1 myeloma cells expressing red fluorescent protein (RFP). CD14 monocytes were the least efficient in heterofusing with KAS 6/1 cells, whereas the mDCs were most efficient (data not shown). The iDCs showed moderate levels of heterofusion with the KAS6/1-RFP cells to yield “yellow” syncytia when viewed using a dual filter under the fluorescence microscope (Fig. 4B).

Monocyte-derived cells can deliver oncolytic measles viruses to myeloma xenografts and prolonged survival of tumor bearing mice

The *in vivo* biodistribution of the monocyte-derived cells after intravenous delivery was tested in SCID mice bearing subcutaneous KAS 6/1 tumors. Monocytes, iDCs, or mDCs were loaded with 250 uCi indium-111 oxine and injected systemically into the mice via the tail vein. The mice were imaged using a micro-SPECT-CT at various time points post–cell delivery. As shown in Fig. 4C, the cells typically arrested transiently in the lungs at the 30 min imaging time point and subsequently trafficked to the liver. There was gradual loss of radioactivity signal over time due to decay of the isotope (physical half-life 2.8 days) and/or loss of cell viability (Fig. 4C). Another cohort of mice was euthanized at 24 hr after infusion of radiolabeled cells and organs were harvested and the amount of radioactivity was measured using a well-type scintillation counter (Fig. 4D). As predicted from the SPECT-CT images, the majority of injected cells accumulated in the liver, whereas there was very little signal (approximately 0.5% of the injected radioactivity) from the KAS 6/1 tumor. Because the animals were given 10^6 cells intravenously, we estimate that approximately 500 cell carriers may have accumulated in the SQ tumors.

Because the iDCs were efficiently infected by the virus, they could heterofuse with KAS 6/1 cells to transfer measles virus and were very robust in terms of cell viability, we chose to concentrate on using them as potential virus carriers. The iDCs were preinfected with MV-Luc or MV-RFP (MOI 1.0) and infused intravenously via the tail vein into SCID mice bearing subcutaneous KAS 6/1 xenografts. Mice were imaged using bioluminescent imaging for evidence of viral transfer (luciferase activity) or tumors were harvested and analyzed using fluorescence microscopy to detect RFP-positive cells or MV-RFP infectious centers. As shown in Fig. 5A, MV-Luc–infected iDCs were readily detected using the Xenogen Bioluminescent Imaging system and many of them arrested transiently in the lungs where they could be detected 30 min post IV infusion but not at later time points (Fig. 5A). Virally encoded luciferase activity in the tumors became apparent by 48 hr after the injection of MV-Luc–infected iDC and increased in intensity over the next few days as MV-Luc spread within the tumor (Fig. 5A). Tissue sections of the myeloma xenografts were immunostained with antibodies to human MHC-II to detect the presence of infiltrating human iDCs at 6 hr post–cell delivery. As shown in Fig. 5B, MHC-II positive uninfected or MV-infected iDCs were detected in the tumor parenchyma. Tumors from mice given MV-RFP–infected iDCs were excised at day 3 post–cell infusion, sectioned into 5-mm slices and examined using the fluorescence microscope (100× magnification). Single RFP-positive MV-infected iDCs were found in tumors (Fig. 5C). In addition, syncytia were also observed in the tumors, signifying spread of MV-RFP from infected iDCs to tumor cells, with subsequent intercellular fusion between infected and uninfected KAS 6/ 1 myeloma cells. Immunostaining for MV-N confirmed the presence of measles infected foci in the tumors (Fig. 5C). Tumors in mice that received uninfected iDCs were not RFP positive and did not stain positive for MV-N (data not shown).

We next sought to determine if virus-infected iDCs could deliver measles virus for the treatment of disseminated disease in an orthotopic myeloma model. Systemic myeloma was established in SCID mice by intravenous delivery of 4×10^6 KAS 6/1 cells. Four weeks later, mice were treated intravenously with 3×10^6 virus-infected iDCs that had been preinfected with a recombinant measles virus (MV-NIS) that is currently undergoing Phase I clinical testing in patients with treatment refractory myeloma. Mice received two doses of treatment, given 1 week apart. Tumor-bearing mice in the saline control group ($n = 20$) exhibited signs of hind limb paralysis, lost more than 10% of body weight, and were euthanized after a median of 40.5 days (Fig. 5D). Uninfected iDC cell carriers had no antimyeloma activity and extension of mice survival was not observed (data not shown). In contrast, the survival of mice in the treatment group was significantly prolonged (median survival 60.5 days, $P < 0.0001$), although

all these mice eventually had to be euthanized due to disease progression and there were no long-term survivors (Fig. 5D).

Discussion

Here, we demonstrate that skeletal plasmacytomas are infiltrated with CD68+, CD163+ macrophages (TAMs) and with CD3+ T lymphocytes. The skeletal plasmacytomas analyzed in this study were obtained from patients with a diagnosis of multiple myeloma. In all cases, the TAMs were distributed uniformly among the neoplastic plasma cells and their density was relatively constant throughout each tumor. The absolute density of infiltration varied between patients from as low as 2% to as high as 12% of nucleated cells per high-power field. Most of the macrophages had clear dendritic morphology with each TAM in contact with numerous myeloma cells. In a small percentage of cases, there was a subpopulation of TAMs that were strikingly clustered around CD34-positive blood vessels. It will be interesting to study the hypothesis that these cells might be contributing to the process of tumor angiogenesis. Bone marrow-resident macrophages from patients with multiple myeloma were recently shown to be capable of vasculogenic mimicry [17]. Careful analysis of the plasmacytoma sections shown in Fig. 3 provides evidence that TAM at this site may also be capable of vascular mimicry. In contrast to the macrophages, the distribution of infiltrating T lymphocytes was highly variable both between patients and within a given tumor, ranging from 0 to 10% of nucleated cells in different high-power fields from a single patient sample.

Cancer therapy using tumor-selective oncolytic viruses has shown promise in clinical trials and a number of virotherapy agents have been tested for antimyeloma therapy including vaccinia virus, coxsackie virus, and vesicular stomatitis virus [18–21]. For several years, we have been developing oncolytic measles viruses as a novel antimyeloma therapeutic modality [22,23]. Attenuated measles viruses are selectively destructive to human myeloma plasma cells and are therapeutically potent in murine myeloma xenograft models [22]. In part, this is because myeloma cells express high levels of the measles receptor CD46, which mediates efficient virus entry and subsequent measles-driven intercellular fusion [24]. A recombinant measles virus, MV-NIS, is currently being tested at Mayo Clinic as an intravenous therapy for patients with advanced, treatment-refractory multiple myeloma in an NCI-sponsored Phase I clinical trial [25]. As a strategy to potentially enhance delivery of MV to myeloma nodules in the bone marrow and to protect the virus from potentially inhibitory factors (complement, antimeasles antibodies) in the circulation, we and others are exploring the use of carrier cells as Trojan horses to deliver viruses to tumors [26–28]. The optimal carrier cell should be highly susceptible to MV infection, not be rapidly killed by the virus, traffic to tumors and transfer the virus infection to the tumor cells via cell to cell heterofusion and/or by production of virus progeny [29,30]. Our immunohistochemical studies suggested that monocytes/dendritic cells might be the ideal carriers for MV delivery into myeloma deposits because of the propensity of monocytes to be recruited into plasmacytomas. The data presented in this article show that this is indeed a highly feasible strategy because MV-infected human iDCs could efficiently traffic from the bloodstream into subcutaneous KAS6/1 plasmacytomas and initiate a spreading measles infection at that site. Furthermore, iDCs loaded with the oncolytic virus MV-NIS were able to prolong mouse survival in the orthotopic KAS6/1 myeloma xenograft model. Tumor regression was not observed in animals treated with uninfected cell carriers. Thus, the mechanism of antimyeloma activity is due to infected iDC cell carriers passing measles virus infection to the tumors, initiating numerous foci of viral infection and spread to result in control of tumor xenograft growth.

It is of interest to consider how TAM accumulate in growing plasmacytomas. The prominence of TAM as components of the stroma of many tumors has led to their extensive study [9,12]. TAM derived from circulating monocyte precursors, which are recruited into tumors from the

circulation under the influence of potent chemotactic signals from the tumor microenvironment [9,31]. These monocytes subsequently differentiate to become TAM but do not proliferate after entering the tumor parenchyma [32]. Several molecules have been implicated in the recruitment and survival of TAMs, the most important being CCL2 whose cognate receptor, CCR2, is expressed abundantly on circulating monocytes [12,31]. CCL2, also known as monocyte chemotactic protein-1 or MCP-1, is an inducible chemokine that is known to be constitutively expressed in many tumors. lnterleukin-6, which plays a central role in the biology of multiple myeloma, was recently shown to potently induce the expression and secretion of CCL2 by myeloma plasma cells [33], suggesting that this chemokine may be key to the intratumoral recruitment of monocytes in patients with multiple myeloma. However, careful studies will be needed to identify the specific role of IL-6 because there are several additional soluble factors in the myeloma microenvironment (vascular endothelial growth factor and M-CSF, for example) known to promote macrophage recruitment, survival, and proliferation [4]. Differences in the intratumoral distribution patterns and TAM morphologies in plasmacytomas from different myeloma patients may also prove to be related to differences in local intratumoral concentrations and concentration gradients of these various chemoattractant factors.

Macrophages are broadly divided into M1 and M2 subtypes [34]. M1 macrophages are proinflammatory, whereas M2 macrophages are immunosuppressive. TAM are M2 macrophages that have been shown in several malignancies to promote tissue repair, angiogenesis, and tumor progression by suppressing adaptive antitumor immune responses, enhancing tumor cell survival, proliferation, invasion, and metastasis, promoting new blood vessel formation, and remodeling of the tumor matrix [12]. Their protu-moral activity is mediated through adhesive interactions with tumor cells or vascular endothelial cells, and through the elaboration of tumor-promoting chemokines, growth factors, and matrix-degrading proteases. Based on the uniform intratumoral distribution of TAMs in these plasmacytomas and intimate dendritic associations with neoplastic plasma cells, it seems highly likely that TAM provide a necessary stimulus to the survival and proliferation of the malignant cells. Given that osteoclasts are key to the paracrine stimulation of myeloma growth at the periphery of expanding plasmacytomas [6,35], it is tempting to speculate that TAM are providing equivalent support functions at sites of myeloma growth where there are no osteoclasts present. TAM, like osteoclasts, are members of the monocytic cell lineage and therefore capable of producing many of the osteoclast-derived factors that have been previously implicated in the maintenance of myeloma cell viability and proliferation [6]. In keeping with this argument, *in vitro* studies have recently reported that dendritic cells can significantly enhance the clonogenicity of several multiple myeloma cell lines and primary tumor cells from patients with multiple myeloma [5]. In addition to enhancing the survival and proliferation of myeloma cells, the subset of TAM that are visibly concentrated around the tumor neovessels may well be contributing to the process of tumor angiogenesis. The vasculogenic properties of bone marrow macrophages from patients with multiple myeloma were recently investigated, leading to the conclusion that these cells are capable of vasculogenic mimicry [17]. Our analysis of plasmacytomas immunostained with antibodies to CD34 and CD68 do provide some support for this conclusion, at least in a small number of tumors, but not in the majority of cases.

Aside from their potential utility as vehicles for the delivery of oncolytic viruses to sites of tumor growth, the identification of TAM as a dominant stromal component in plasmacytomas can potentially be exploited in other ways to improve the outcomes of myeloma therapy. Indeed, myeloma drug discovery efforts are being focused increasingly on the microenvironment [36]. Future approaches suggested by our findings may include the development of drugs that can block key interactions between TAM and myeloma cells (eg, LFA-1 binding to ICAM-1), or that can convert the TAM from their M2 phenotype to a proinflammatory M1 phenotype. Alternatively, the powerful ability of plasmacytomas to

recruit TAM provides an opportunity to exploit the monocytic lineage as delivery vehicles to carry alternative therapeutic agents into these sites of tumor growth.

In summary, we have shown that the plasmacytomas of myeloma patients are heavily infiltrated with TAM and that cells of the monocytic lineage can be exploited as cell carriers to transport oncolytic viruses to sites of myeloma growth. Plasmacytoma-infiltrating TAM should be further studied to determine their role in supporting myeloma growth because this mechanistic information may provide additional potential opportunities for the development of novel approaches to myeloma therapy.

Materials and Methods

Immunostaining

Archived paraffin-embedded tissues from 22 plasmacytoma biopsies obtained from patients previously diagnosed with MM at the Mayo Clinic were studied. All biopsy specimens were obtained from plasmacytomas. Each case was either stained with H&E or with antibodies directed against CD3 (Novocastra, clone PS1), CD68 (Dako, clone PGM-1), CD163 (Novocastra, clone 10D6), the dendritic cell marker S100 or the vascular marker CD34 (Becton Dickinson, clone MY10) [37]. Antigen retrieval was performed in a heated 1 mM EDTA pH 8.0 solution for 30 min. Antigen–antibody reactions were visualized using a polymer-based detection system (Dako, Capinteria, CA) using diaminobenzidine (DAB) as the chromogen. The cases were also double stained for CD68 (Fast Red)/CD34 (DAB) using the Envision Doublestain System (Dako). Slides were viewed on an Olympus BX51 microscope and images were captured using an Olympus DP70 digital camera. Percentage infiltration by CD68-positive or CD3-positive cells was determined by counting the numbers of stained and unstained cells in 10 representative high-power fields (400×) for each plasmacytoma section.

Human KAS 6/1 or MM1 myeloma xenografts grown in SCID mice were snap frozen in OCT and 5 μm sections were obtained. The tumor sections were fixed in acetone (−20°C) for 10 min, air-dried, and permeabilized using 0.01% Triton-X in phosphate-buffered saline (PBS) for 10 min. Endogenous phosphatase activity was quenched using 20% acetic acid for 15 min at 4°C, washed and blocked with blocking buffer containing 5% horse serum in PBS for 30 min. Tissues were incubated with biotinylated rat anti-murine CD68 antibody (AbD Serotec, 1:200 dilution) for 1 hr at room temperature, washed five times in PBS, incubated with ABC standard kit for HRP (Vector Labs) for 30 min, washed in PBS and developed with Vector Labs DAB substrate kit per manufacturer's instructions.

For staining of human DC infiltrate in KAS tumors in mice, the tumor sections were probed with mouse anti-MHC Class II antibody (Affinity Bioreagents, 1:50 dilution) for 1 h at room temperature, followed by incubation with Cy3 conjugated anti-mouse antibody (Chemicon, 1:1500) for 15 min.

Purification and maturation of primary CD14 cells

Cells retained in the leukoreduction system chambers after apheresis of normal platelet donors were collected, diluted with PBS and layered over Lymphoprep density gradient solution [38]. To isolate CD14+ cells, 200 μL of CD14-specific immunomagnetic reagent (Miltenyi Biotec, Auburn, CA) was incubated with 4×10^8 PBMNCs resuspended in 1.6 ml PBSFE. After incubation and washing, the labeled cells were separated on a separator (AutoMACS, Miltenyi Biotec) running the POSSEL program. Purity of isolated cells was accessed by flow cytometry with anti-CD14 antibodies. The CD14+ monocytes were used immediately in infection assays or cultured as described previously [39,40]. Briefly, 9.0×10^6 immunomagnetically purified CD14+ cells were seeded in six-well plates in 3 ml of Stemliine

DC medium (Sigma–Aldrich, St Louis, MO) supplemented with 2 mM L-glutamine, GM-CSF, 1000 lU/mL (Berlex, Montville, NJ) and 1.0% penicillin-streptomycin (Gibco, Grand Island, NY) for 3 days in a 37°C 5%CO_2 humidified incubator. These nonadherent immature DCs (iDCs) were either harvested on day 3 postplating for use in infection assays or matured further in fresh Stemline DC maturation medium containing 1000 lU/ml GM-CSF, 1100 lU/mL tumor necrosis factor-α (R&D Systems, Minneapolis, MN) and 1.0 μg/mL PGE2 (Sigma–Aldrich). On Day 5, nonadherent mDCs were collected by centrifugation and used in infection assays.

Construction of MV-RFP virus and virus infection assays

Attenuated Edmonston strain measles virus expressing enhanced GFP (MV-eGFP), or RFP (MV-RFP) or firefly luciferase (MV-Luc) were propagated on African green monkey kidney Vera cells as described previously [29]. The MV-RFP full length infectious cDNA of MV was constructed by inserting the cDNA of RFP in position 1 upstream of the MV nucleocapsid (N) gene of MV-eGFP as a Mlu l-Aat II insert [41]. The MV-RFP was rescued on 293-3-46 cells and propagated to titers comparable to MV-eGFP and MV-Luc (10^7 $TCID_{50}$/ml).

Monocytes, iDCs, or mDCs were infected with MV-eGFP or MV-RFP at MOI of 1.0 for 2 hr in reduced serum medium, Opti-MEM (Invitrogen), after which the inoculum was removed and the cells were maintained in standard medium containing a FIR Forty-eight hours later, the cells were harvested, fixed in PBS containing 4% paraformaldehyde and the percentage of fluorescent single infected cells were analyzed by flow cytometry (FACScan, Becton Dickinson, San Jose, CA). For heterofusion assays, MV-Luc–infected or mock–infected monocytes, iDCs, or mDCs were labeled with a lipophilic dye (DiO, Molecular Probes) and mixed with RFP-expressing KAS 6/1 cells. The cocultures were observed daily and photographs were taken using a fluorescence microscope.

In vivo studies

Four- to 5-week-old female SCID mice (Harlan Sprague–Dawley, Indianapolis, IN) were given whole body irradiation (150 rads) and inoculated subcutaneously in the right flank with 1×10^7 human myeloma KAS 6/1 cells. Tumors typically took 6–8 weeks for diameters to reach 0.5 cm. CD14, iDC, or mDC were labeled with indium-111 oxine (250 uCi) for 20–30 min after which cells were washed and infused intravenously into mice with SQ tumors. Mice were imaged at various time intervals using a micro SPECT-CT (Gamma Medica, Northridge, CA) and images were analyzed using the AMIRA software. Major organs and SQ tumors were harvested and the scintillation counts were determined using a well-type scintillation counter. To track transfer of MV by cell carriers, another cohort of mice were given 10^6 iDCs preinfected 18 hr earlier with MV-Luc or MV-RFP (MOI 1.0). Bioluminescent imaging was performed on the mice at various time points post-iDC infusion using the Xenogen IVIS 200 machine (Alameda, CA) and images were analyzed using the Living Systems 2.5 software. Tumors from mice that received MV-RFP infected iDCs were harvested, snap frozen for immunohistochemistry or sliced into 5-mm sections using a razor blade and examined under a fluorescence microscope (Nikon Eclipse E400). Images of the fresh tissues were captured using a high-resolution Nikon digital camera (DXM1200) and ACT-1 software (Nikon Instruments, Melville, NY). Confocal microscopy of immunostained cryosections of tumors (5 μm thickness) were performed using a Zeiss LSM 510 confocal laser scanning Axiovert inverted microscope (Oberkochen, Germany). For the therapy experiment, disseminated myeloma disease was established in 5-week-old SCID mice that had been irradiated with 150 cGy 1 day before to improve tumor implantation. A total of 4×10^6 KAS 6/1 cells were given intravenously via the tail vein. Four weeks post KAS 6/1 cell implantation, mice were divided into two cohorts and given saline (n = 20 mice) or MV-NIS infected iDC (n = 15 mice). The iDC were preinfected with MV-NIS (MOI 2.0) 1 day before use, washed the next day and

infused intravenously via the tail (3×10^6 cells/mouse/100 μl). Mice received two doses of treatment given 1 week apart.

Acknowledgments

Contract grant sponsor: NIH/NCI, Charlotte-Geyer Foundation, and Alliance for Cancer Gene Therapy; Contract grant number: CA100634, CA129996.

References

1. Kyle RA. Multiple myeloma: An odyssey of discovery. Br J Haematol 2000;111:1035–1044. [PubMed: 11167737]
2. Rosinol L, Blade J, Esteve J, et al. Smoldering multiple myeloma: Natural history and recognition of an evolving type. Br J Haematol 2003;123:631–636. [PubMed: 14616966]
3. Said JW, Rettig MR, Heppner K, et al. Localization of Kaposi's sarcoma-associated herpesvirus in bone marrow biopsy samples from patients with multiple myeloma. Blood 1997;90:4278–4282. [PubMed: 9373238]
4. Hideshima T, Mitsiades C, Tonon G, et al. Understanding multiple myeloma pathogenesis in the bone marrow to identify new therapeutic targets. Nat Rev Cancer 2007;7:585–598. [PubMed: 17646864]
5. Kukreja A, Hutchinson A, Dhodapkar K, et al. Enhancement of clonogenicity of human multiple myeloma by dendritic cells. J Exp Med 2006;203:1859–1865. [PubMed: 16880256]
6. Roodman GD. Myeloma bone disease: Pathogenesis and treatment. Oncology (Williston Park) 2005;19:983–984. 986. [PubMed: 16131042]
7. Rajkumar SV, Mesa RA, Fonseca R, et al. Bone marrow angiogenesis in 400 patients with monoclonal gammopathy of undetermined significance, multiple myeloma, and primary amyloidosis. Clin Cancer Res 2002;8:2210–2216. [PubMed: 12114422]
8. Bingle L, Brown NJ, Lewis CE. The role of tumour-associated macrophages in tumour progression: Implications for new anticancer therapies. J Pathol 2002;196:254–265. [PubMed: 11857487]
9. Pollard JW. Tumour-educated macrophages promote tumour progression and metastasis. Nat Rev Cancer 2004;4:71–78. [PubMed: 14708027]
10. Ohno S, Suzuki N, Ohno Y, et al. Tumor-associated macrophages: Foe or accomplice of tumors? Anticancer Res 2003;23:4395–4409. [PubMed: 14666727]
11. Lewis CE, Pollard JW. Distinct role of macrophages in different tumor micro-environments. Cancer Res 2006;66:605–612. [PubMed: 16423985]
12. Sica A, Schioppa T, Mantovani A, et al. Tumour-associated macrophages are a distinct M2 polarised population promoting tumour progression: Potential targets of anti-cancer therapy. Eur J Cancer 2006;42:717–727. [PubMed: 16520032]
13. Ishigami S, Natsugoe S, Tokuda K, et al. Tumor-associated macrophage (TAM) infiltration in gastric cancer. Anticancer Res 2003;23:4079–4083. [PubMed: 14666722]
14. Dirkx AE, Oude Egbrink MG, Wagstaff J, et al. Monocyte/macrophage infiltration in tumors: Modulators of angiogenesis. J Leukoc Biol 2006;80:1183–1196. [PubMed: 16997855]
15. Vallario A, Chilosi M, Adami F, et al. Human myeloma cells express the CD38 ligand CD31. Br J Haematol 1999;105:441–444. [PubMed: 10233418]
16. Bhatti SS, Kumar L, Dinda AK, et al. Prognostic value of bone marrow angiogenesis in multiple myeloma: Use of light microscopy as well as computerized image analyzer in the assessment of microvessel density and total vascular area in multiple myeloma and its correlation with various clinical, histological, and laboratory parameters. Am J Hematol 2006;81:649–656. [PubMed: 16845660]
17. Scavelli C, Nico B, Cirulli T, et al. Vasculogenic mimicry by bone marrow macrophages in patients with multiple myeloma. Oncogene 2007;27:663–674. [PubMed: 17667938]
18. Stief AE, McCart JA. Oncolytic virotherapy for multiple myeloma. Expert Opin Biol Ther 2008;8:463–473. [PubMed: 18352850]
19. Deng H, Tang N, Stief AE, et al. Oncolytic virotherapy for multiple myeloma using a tumour-specific double-deleted vaccinia virus. Leukemia 2008;22:2261–2264. [PubMed: 18509356]

20. Au GG, Lincz LF, Enno A, et al. Oncolytic coxsackievirus A21 as a novel therapy for multiple myeloma. Br J Haematol 2007;137:133–141. [PubMed: 17391493]
21. Lichty BD, Stojdl DF, Taylor RA, et al. Vesicular stomatitis virus: A potential therapeutic virus for the treatment of hematologic malignancy. Hum Gene Ther 2004;15:821–831. [PubMed: 15353037]
22. Peng KW, Ahmann GJ, Pham L, et al. Systemic therapy of myeloma xenografts by an attenuated measles virus. Blood 2001;98:2002–2007. [PubMed: 11567982]
23. Dingli D, Peng KW, Harvey ME, et al. Image-guided radiovirotherapy for multiple myeloma using a recombinant measles virus expressing the thyroidal sodium iodide symporter. Blood 2004;103:1641–1646. [PubMed: 14604966]
24. Ong HT, Timm MM, Greipp PR, et al. Oncolytic measles virus targets high CD46 expression on multiple myeloma cells. Exp Hematol 2006;34:713–720. [PubMed: 16728275]
25. Myers RM, Greiner SM, Harvey ME, et al. Preclinical pharmacology and toxicology of intravenous MV-NIS, an oncolytic measles virus administered with or without cyclophosphamide. Clin Pharmacol Ther 2007;82:700–710. [PubMed: 17971816]
26. Thorne SH, Contag CH. Integrating the biological characteristics of oncolytic viruses and immune cells can optimize therapeutic benefits of cell-based delivery. Gene Ther 2008;15:753–758. [PubMed: 18356814]
27. Munguia A, Ota T, Miest T, et al. Cell carriers to deliver oncolytic viruses to sites of myeloma tumor growth. Gene Ther 2008;15:797–806. [PubMed: 18356812]
28. Power AT, Wang J, Falls TJ, et al. Carrier cell-based delivery of an oncolytic virus circumvents antiviral immunity. Mol Ther 2007;15:123–130. [PubMed: 17164783]
29. Ong HT, Hasegawa K, Dietz AB, et al. Evaluation of T cells as carriers for systemic measles virotherapy in the presence of antiviral antibodies. Gene Ther 2007;14:324–333. [PubMed: 17051248]
30. Iankov ID, Blechacz B, Liu C, et al. Infected cell carriers: A new strategy for systemic delivery of oncolytic measles viruses in cancer virotherapy. Mol Ther 2007;15:114–122. [PubMed: 17164782]
31. Mantovani A, Allavena P, Sozzani S, et al. Chemokines in the recruitment and shaping of the leukocyte infiltrate of tumors. Semin Cancer Biol 2004;14:155–160. [PubMed: 15246050]
32. Mantovani A, Bottazzi B, Colotta F, et al. The origin and function of tumor-associated macrophages. Immunol Today 1992;13:265–270. [PubMed: 1388654]
33. Arendt BK, Velazquez-Dones A, Tschumper RC, et al. Interleukin 6 induces monocyte chemoattractant protein-1 expression in myeloma cells. Leukemia 2002;16:2142–2147. [PubMed: 12357369]
34. Mantovani A, Sica A, Locati M. Macrophage polarization comes of age. Immunity 2005;23:344–346. [PubMed: 16226499]
35. Yaccoby S, Wezeman MJ, Henderson A, et al. Cancer and the microenvironment: Myeloma–osteoclast interactions as a model. Cancer Res 2004;64:2016–2023. [PubMed: 15026338]
36. Anderson KC. Targeted therapy of multiple myeloma based upon tumor-microenvironmental interactions. Exp Hematol 2007;35:155–162. [PubMed: 17379101]
37. Dogan A, Burke JS, Goteri G, et al. Micronodular T-cell/histiocyte-rich large B-cell lymphoma of the spleen: Histology, immunophenotype, and differential diagnosis. Am J Surg Pathol 2003;27:903–911. [PubMed: 12826882]
38. Dietz AB, Bulur PA, Emery RL, et al. A novel source of viable peripheral blood mononuclear cells from leukoreduction system chambers. Transfusion 2006;46:2083–2089. [PubMed: 17176319]
39. Dietz AB, Bulur PA, Erickson MR, et al. Optimizing preparation of normal dendritic cells and bcr-abl+ mature dendritic cells derived from immunomagnetically purified CD14+ cells. J Hematother Stem Cell Res 2000;9:95–101. [PubMed: 10738977]
40. Dietz AB, Padley DJ, Butler GW, et al. Clinical-grade manufacturing of DC from CD14+ precursors: Experience from phase I clinical trials in CML and malignant melanoma. Cytotherapy 2004;6:563–570. [PubMed: 15773024]
41. Duprex WP, McQuaid S, Roscic-Mrkic B, et al. In vitro and *in vivo* infection of neural cells by a recombinant measles virus expressing enhanced green fluorescent protein. J Virol 2000;74:7972–7979. [PubMed: 10933705]

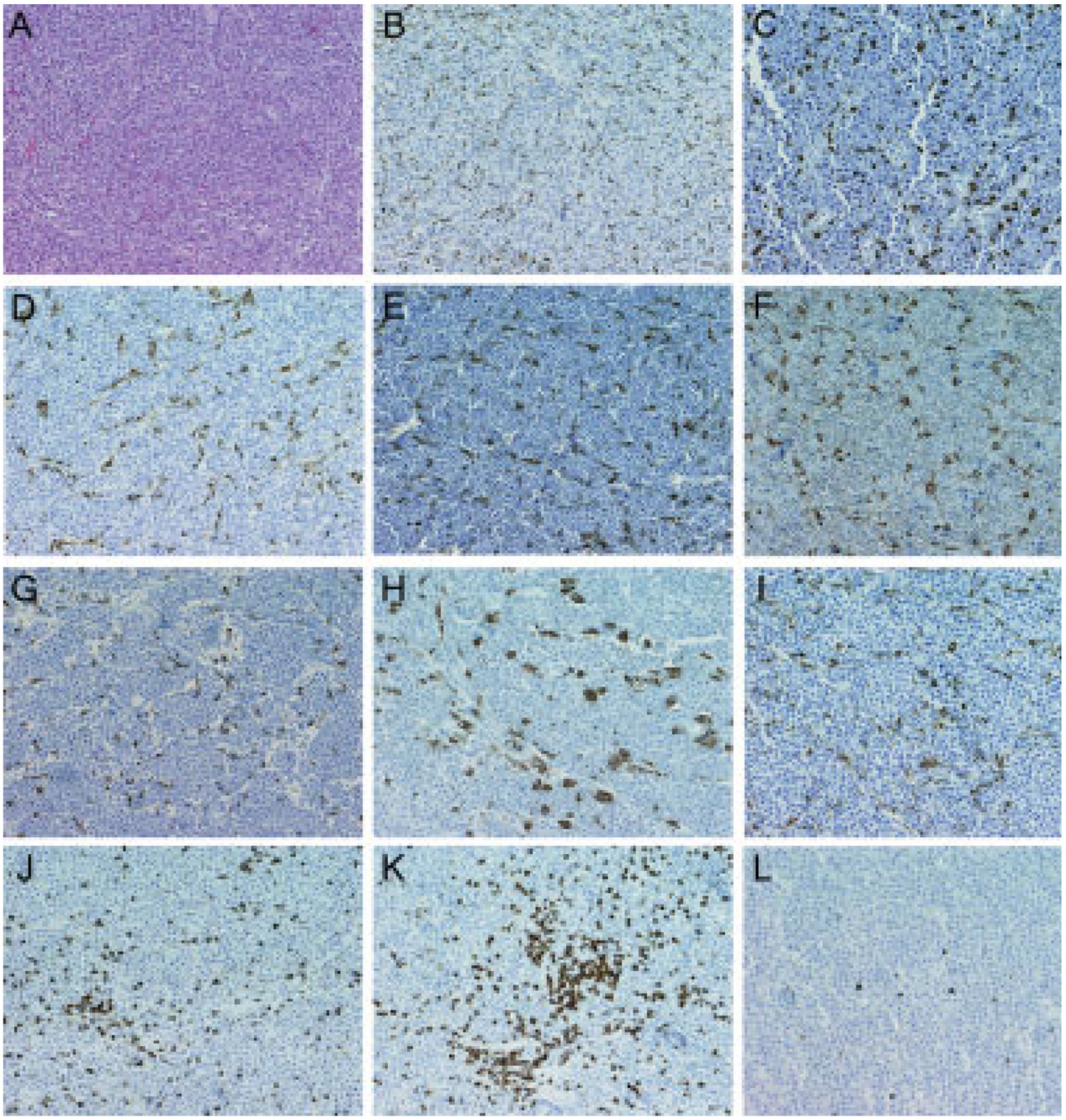

Figure 1.
Leukocyte infiltrates in plasmacytomas from multiple myeloma patients. (A) Hematoxylin and eosin stained, (B–I) CD68 immunostained or (J–L) CD3 immunostained paraffin sections of plasmacytomas from representative cases. All immunostained slides were counterstained with hematoxylin. Note that, in general, the CD68 cells are uniformly dispersed within the plasmacytoma, whereas some of the CD3 cells are found in clusters. Original magnification is 200×.

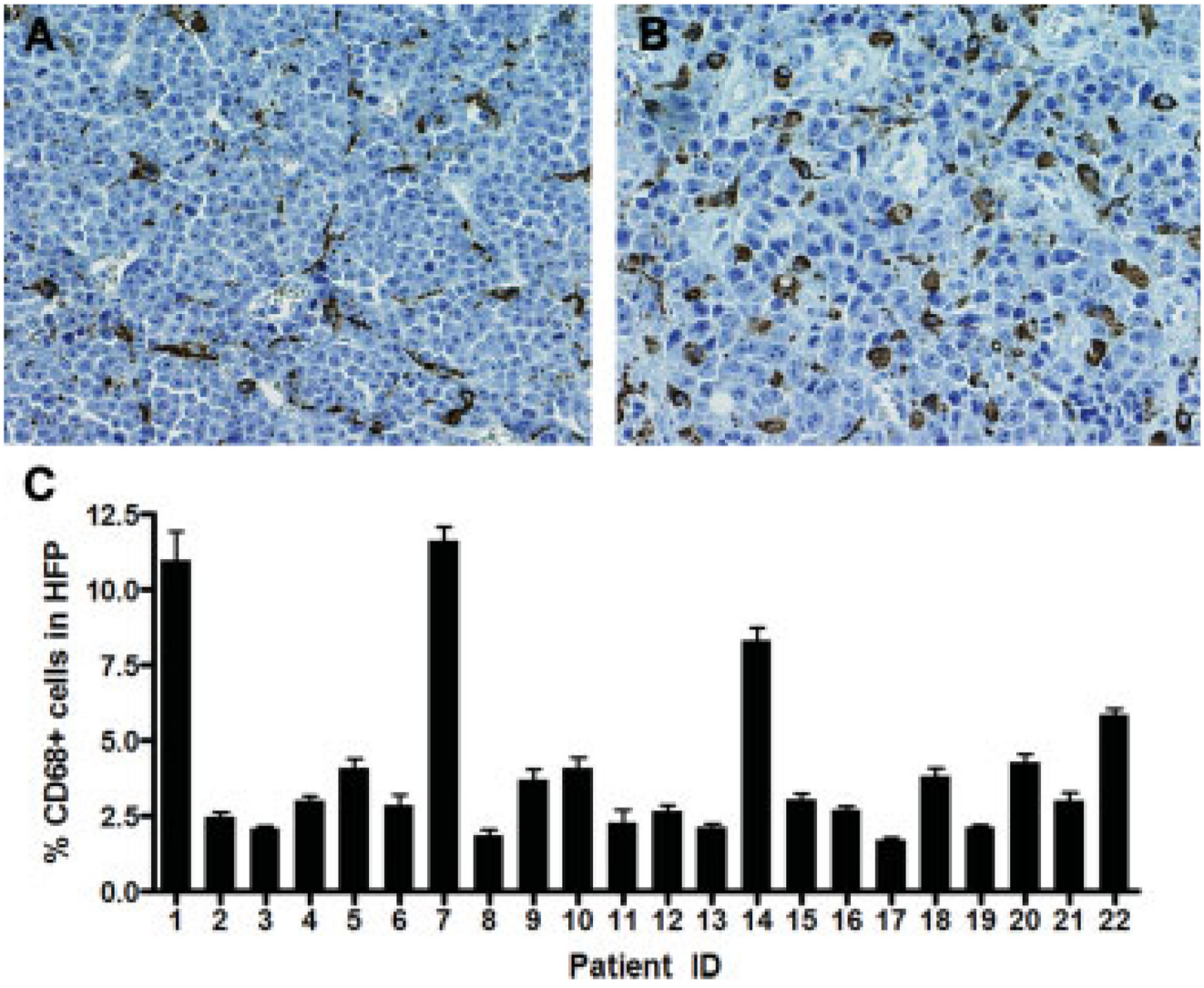

Figure 2.

Quantitation of CD68+ infiltrates in plasmacytomas. (A) Representative high-power fields (HPF, 400× magnification) showing images from two different plasmacytoma cases immunostained with anti-CD68. Note the dendritic morphology of the macrophages. (B) Percentage of CD68-positive cells in the 22 cases of plasmacytomas examined. Numbers of CD68-positive cells in 10 representative HPFs were counted for each case and expressed as a percentage of the total number of nucleated cells in the same field. Error bars represent the SD about the mean (n = 10 HPFs).

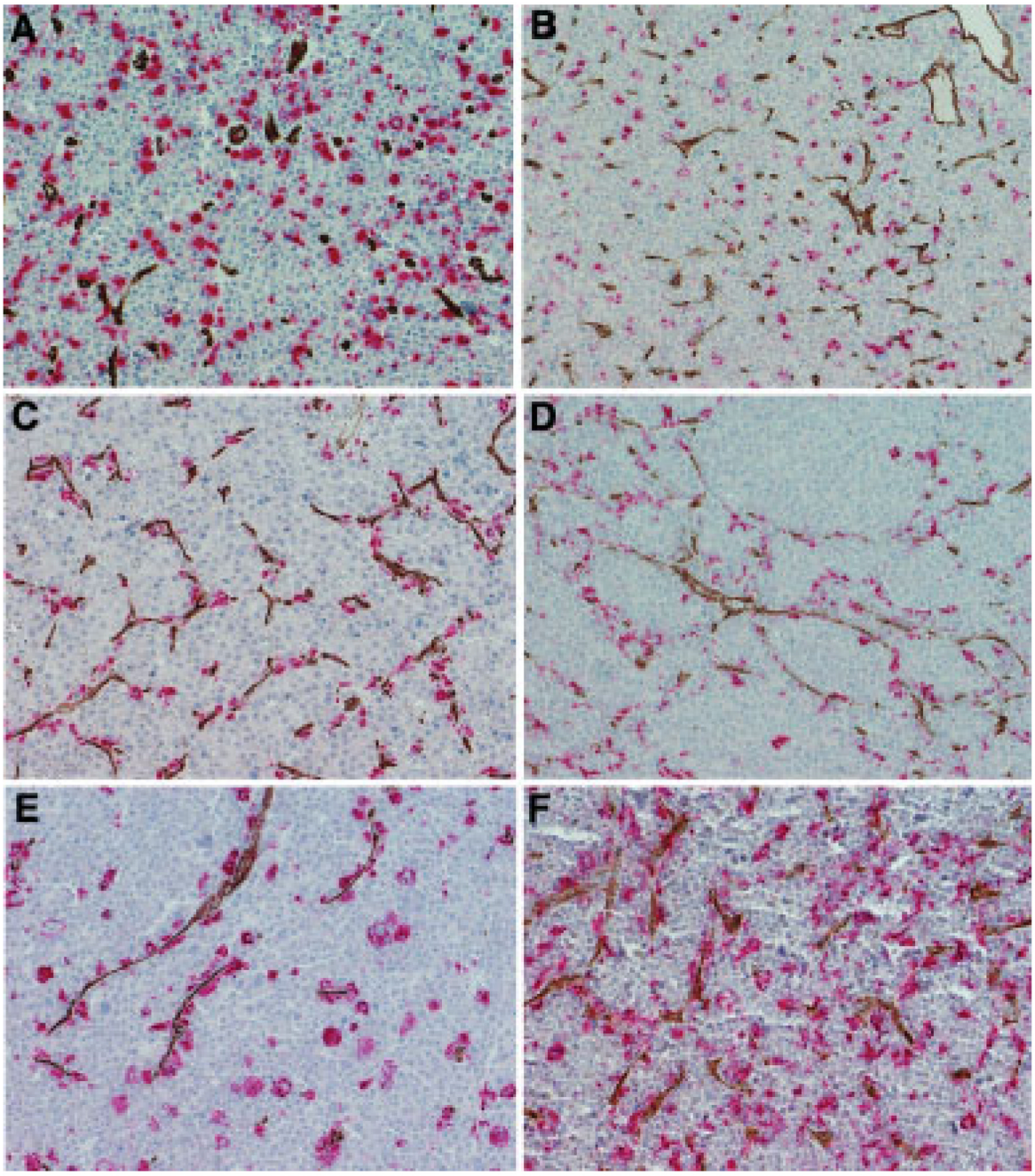

Figure 3.

Spatial relationship between tumor-associated macrophages (TAM) and tumor blood vessels. Plasmacytomas were dual stained with anti-CD68 (Fast red, red staining) and anti-CD34 (DAB, brown staining) antibodies to detect TAMs and tumor blood vessels, respectively. (A and B) Representative examples showing independent distributions of CD68 macrophages and tumor blood vessels. Here, the TAM are not associated with the blood vessels. This pattern was observed in the majority of the cases. (C and D) Examples in which the TAM are closely associated with the CD34 blood vessels with evidence of vascular mimicry. (D and F) Two patterns of TAM distribution are seen in these examples. Here, one population of TAM is

distributed randomly and another population is closely associated with the blood vessels. Original magnification is 200×.

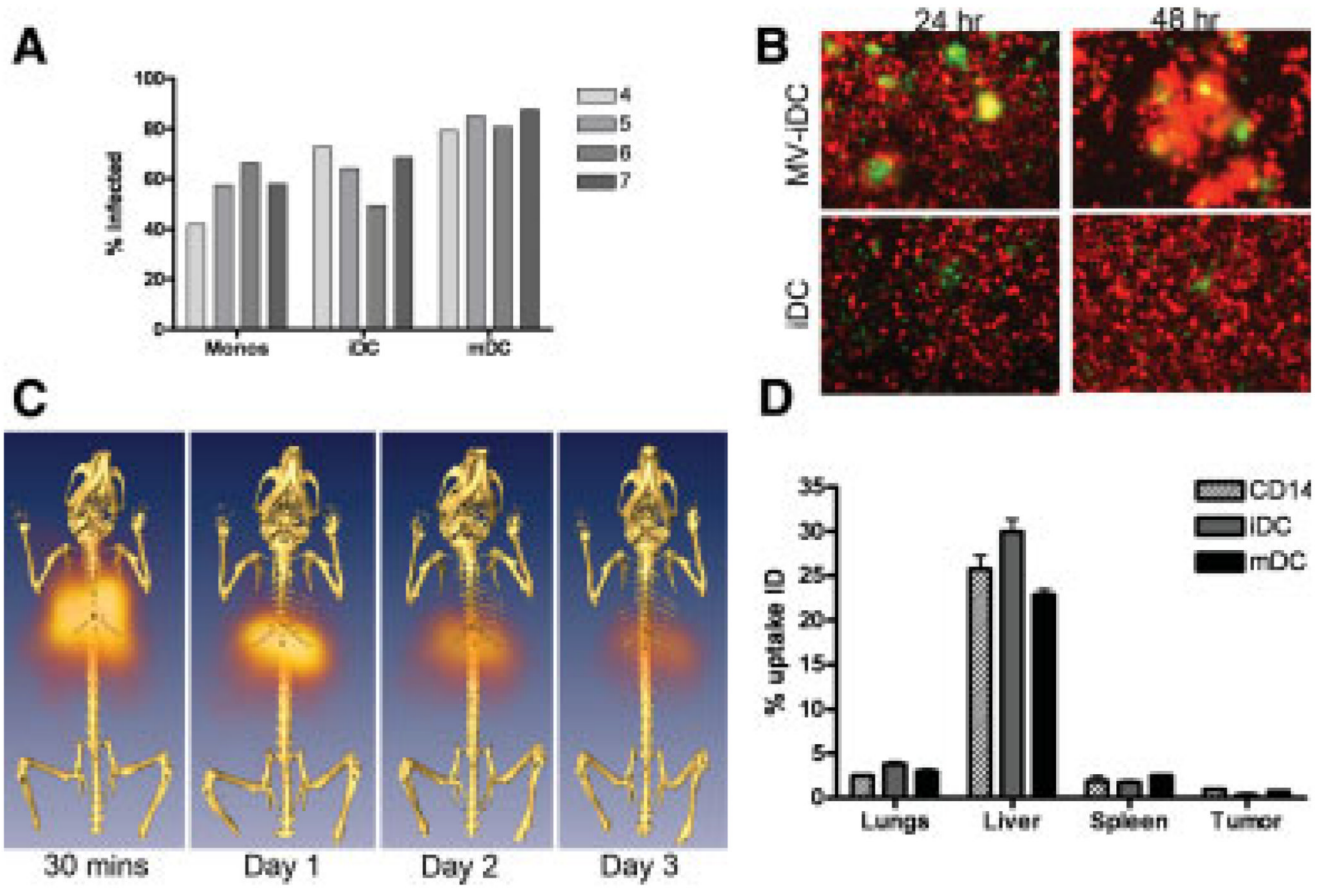

Figure 4.

Potential use of monocytes and dendritic cells (DC) as virus-infected cell carriers. (A) Susceptibility of CD14+ monocytes, iDCs, and mDCs from four blood donors to infection by MV-eGFP. Percentage of infected GFP-positive cells was analyzed by flow cytometry at 48 hr postinfection. (B) Heterofusion of MV-Luc–infected DiO (green)-labeled iDCs with RFP-expressing (red) human KAS 6/1 myeloma cells in culture, resulting in syncytium formation at 24 and 48 hr post– cell mixing. Mock infected iDC were used as controls (lower panels). (C) Serial SPECT-CT images of a mouse that has received an intravenous dose of Indium-111 labeled iDC from 30 min to Day 3 post–cell delivery. (D) Scintillation counts (counts per minute) in the respective organs of mice that received an intravenous dose of lndium-111 labeled CD14, iDC, or mDC at 24 hr post–cell delivery. The amount of radioactivity in the respective organs was calculated as a percentage of the radioactivity present in the whole animal at 24 hr.

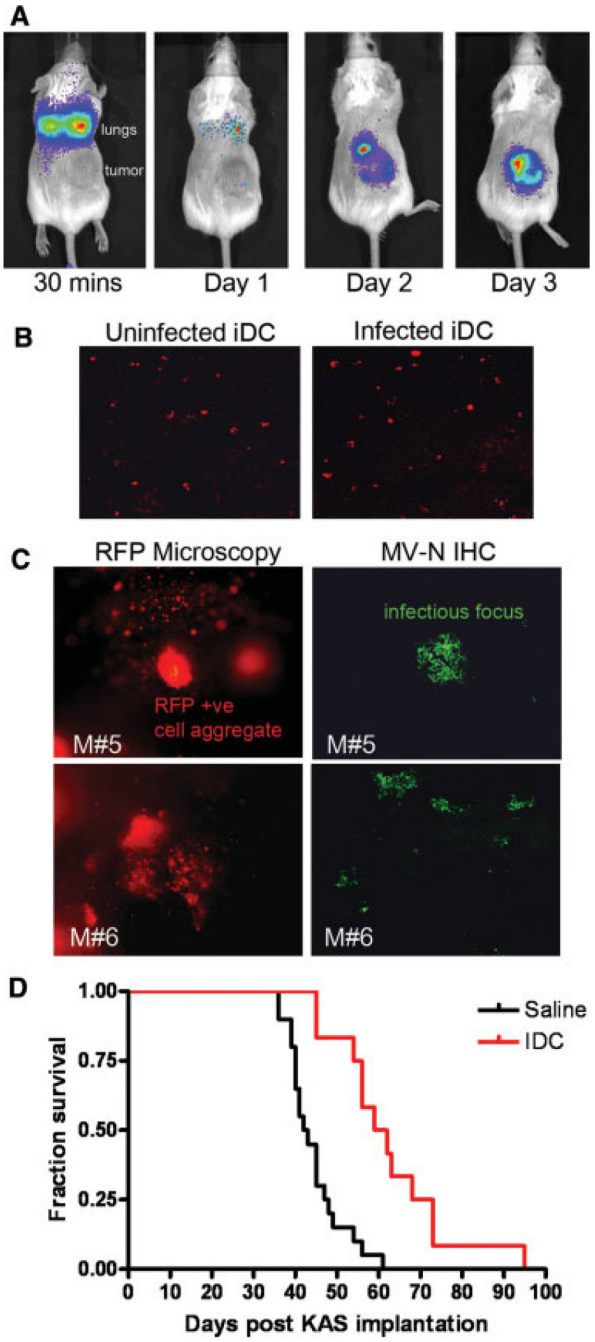

Figure 5.

Adoptively transferred iDC delivered MV to myeloma tumors and extended survival of mice with systemic myeloma disease. (A) Serial bioluminescent imaging of a SCID mouse given one intravenous dose of 1×10^6 MV-Luc–infected iDCs at various time intervals. The positions of the lungs and subcutaneous KAS 6/1 tumor xenograft are noted. (B) Confocal microscope images of tumors harvested from mice that received uninfected or MV-infected iDCs at 6 hr postadoptive transfer of iDCs. The tissue sections were stained with anti-MHC II antibody (red staining) to detect human iDCs. Magnification is 200×. (C) Gross examination of tumors from two different mice (M#5, M#6) harvested 3 days postinfusion of MV-RFP–infected iDCs revealed the presence of single RFP-positive infected iDCs and RFP-positive syncytia. Freshly

harvested tumors were cut into 5-mm slices and photos were taken using a Nikon fluorescence microscope. Magnification is 100×. Immunohistochemical staining for MV-N protein (green, Alexa-488) in 5-μm cryosections confirmed the presence of MV infection in the tumor sections. Note the green infectious foci of MV infection. Magnification is 200×. (D) Kaplan–Meier survival curve of SCID mice bearing systemic KAS 6/1 tumors. Mice received two doses of saline (n = 20 mice) or MV-NIS–infected iDC (n = 15 mice), given 1 week apart.